



Fabrication of PS-TiO₂ hybrid via mini-emulsion polymerization: Study the effect of crosslink on the photocatalytic properties of the hybrid

Thanapong Phetsombun¹, Tanapak Metanawin¹ and Siripan Metanawin^{2,3*}

¹Department of Materials and Production Technology Engineering, Faculty of Engineering, King Mongkut's University of Technology North Bangkok, Bangkok 10800, THAILAND

²Department of Textile Engineering, Faculty of Engineering, Rajamangala University of Technology Thanyaburi, Pathum Thani 12110, THAILAND

³Materials Design and Development (AMDD) Research Unit, Faculty of Engineering, Rajamangala University of Technology Thanyaburi, Pathum Thani 12110, THAILAND

*Corresponding author: siripan.m@en.rmutt.ac.th

ABSTRACT

In this study, a polystyrene (PS)/nano-TiO₂ hybrid was prepared by a mini-emulsion polymerization process to improve the photocatalytic properties when the crosslinking agent was added. *N, N'*-methylenebis (acrylamide) (MBA) was used as a crosslinking agent. The effect of a crosslinking agent on the photocatalytic properties was studied. The diameter, morphology, and photocatalytic properties of the samples were characterized and discussed. The methylene blue discoloration was monitored at 660 nm by a spectrophotometer. The result showed that the L* value from the Hunter color scale for 7 wt% TiO₂-PS/0.25 wt% MBA was highest at 73.73. It was noticed that the 7 wt% TiO₂-PS/0.25 wt% MBA hybrid gave the highest photocatalytic properties. The FE-SEM confirmed the well-defined structure with a spherical shape and network formation to improve the photocatalytic properties. The diameter and morphology of the PS/TiO₂ hybrid were in the range of 76 nm to 95 nm by using a field emission scanning electron microscope (FE-SEM). The particle size of the 1 wt% TiO₂-PS/0.25 wt% MBA was 76 nm, which was smaller than that of the pristine PS of 88 nm. The particle size of the 7 wt% TiO₂-PS/0.25 wt% MBA hybrid was increased by 25%. The HR-TEM image of the PS/TiO₂ hybrid was studied to confirm the encapsulation of TiO₂ particles in the hybrid. The FFT image of PS/MBA/TiO₂ 7 wt% demonstrated the crystalline structure of TiO₂ (dot) and the amorphous structure of PS (ring). FT-IR spectroscopy confirmed the presence of the Ti-O functional group in the PS hybrid spectra. It was noticed that the TiO₂ particles were successfully encapsulated in the PS/TiO₂ hybrid.

Keywords: Mini-emulsion polymerization, Hybrid, Crosslinking agents, Photocatalytic properties

INTRODUCTION

Inorganic-organic nanocomposites in which inorganic (metal oxide) fillers are uniformly dispersed in a polymer matrix have developed strength, toughness, processability, dimensional stability, and wear properties [1-4]. The properties of polymer nanocomposites are affected by the type, size, shape, and concentration of incorporated particles, as well as their interaction with the polymer [5-7].

Polymer hybrids are versatile materials in inorganic-organic nanocomposites. It was the combination of two types of polymers and inorganic nanoparticles to generate advanced materials with possessing properties [8-11]. Therefore, hybrids have been successfully used for various stable inorganic colloids free from aggregation, such as titanium oxide, zinc oxide, magnetic and metal nanoparticles. Mini-emulsion polymerization is one of the common methods for preparing polymer hybrids in colloid systems [12-17].

Titanium dioxide is a widely studied material due to its unique optical, electrical, and chemical properties. It is well-known for its photovoltaic and photocatalytic properties, along with its applications in the paint, paper, and food industries as pigment, filler, or whitener [18-20]. In order to improve the photocatalytic behavior, it is necessary to modify the surface of TiO₂ nanoparticles [21]. This work aimed to synthesize and characterize a novel hybrid material based on TiO₂ nanoparticles. The TiO₂ particles were modified through a mini-emulsion polymerization process in order to improve the surface area and photocatalytic behavior.

MATERIALS AND METHODS

Materials

Styrene monomer (99%, Sigma-Aldrich) was purified by passing through aluminum oxide before

being used. Titanium dioxide (TiO₂ 99%, US Research Nanomaterials), aluminum oxide basic (Al₂O₃, Sigma-Aldrich), hexadecane (HD, 99%, Sigma-Aldrich), sodium dodecyl sulfate (SDS, 99%, Sigma-Aldrich), potassium persulfate (KPS, 99%, Sigma-Aldrich), and *N, N'*-methylenebis (acrylamide) (MBA, 99%, Sigma-Aldrich) were used as received. Deionized water (DI water) was purified by a Micra™ water purifier from ELGA LabWater.

Preparation of polystyrene hybrids

The mini-emulsion polymerization of the polystyrene hybrid was synthesized as follows: 5.00 g of styrene monomer and 0.20 g of hexadecane were mixed in the presence/absence of 0.25 g of MBA. 0.06 g of SDS was dispersed in 20.0 cm³ of water. Then, the dispersion was mixed with the monomer mixture in the flask and stirred under nitrogen gas for 15 minutes. The flask was sonicated (130 W and 60% amplitude) in an ice bath for 15 minutes. After raising the mini-emulsion temperature to 70 °C, 0.083 g of KPS was injected into the flask. The reaction time was carried out for 4 hours. The mini-emulsion was achieved by cooling in an ice bath. The experimental details for the syntheses of PS and PS/MbA/TiO₂ are given in Table 1.

Table 1 The experimental details of the syntheses of PS and PS/MbA/TiO₂.

Sample name	MbA (% wt)	TiO ₂ (% wt)
PS	-	-
PS/TiO ₂ 10%	-	10
PS/MbA	0.25	-
PS/MbA/TiO ₂ 1%	0.25	1
PS/MbA/TiO ₂ 3%	0.25	3
PS/MbA/TiO ₂ 7%	0.25	7
Neat TiO ₂	-	10

Characterization

1. Fourier-transform infrared spectroscopy (FT-IR)

The functional and bonding structures of the PS hybrid were analyzed using a PerkinElmer Frontier spectrometer from the USA. The samples were performed in the range of 4000-400 cm⁻¹.

2. Field Emission Scanning electron microscope (FE-SEM)

The morphology of the PS hybrid was observed on a Jeol JSM-7600F from Japan. The particle size distribution was measured using ImageJ software.

3. High-resolution Transmission electron microscope (HR-TEM)

The morphology and crystalline structure of the PS hybrid were determined on a Jeol JEM-3100F from Japan.

Photocatalytic behavior

The photocatalytic activity of the PS hybrid was examined by observing the discoloration of MB under UV-A (365 nm) TL-K 40W/10-R light from the

Netherlands. 1 mL of PS hybrids was prepared in 10 ppm of the MB solution. The samples were tested without purification. The UV light intensity was 6.0 mW/cm². The MB discoloration was monitored at 660 nm using an UltraScan Pro Color spectrophotometer with a 512-element diode array (from HunterLab, USA).

RESULTS AND DISCUSSION

FT-IR spectroscopy was employed to analyze the functional group and bonding of the PS hybrid. Figure 1 presents the FT-IR spectra of PS, PS/MbA/TiO₂ with various 1, 3, and 7 wt% of TiO₂ contents. It was found that the broad peak at 3423 cm⁻¹ corresponds to the stretching of the surface hydroxyl or absorbed water [22, 23]. The main absorption bands of PS over the 2800-3100 cm⁻¹ range were attributed to C-H stretching vibrations in the main chain and aromatic rings [23]. The absorption bands at 3025, 3063, 3084, 1600, and 1492 cm⁻¹ were assigned to aromatic ring vibrations. The absorption bands at 2921, 2848, and 1451 cm⁻¹ were ascribed to the aliphatic backbone of the polystyrene macromolecule. The characteristic absorption bands of Ti-O particles were observed at 692 cm⁻¹ [22]. It was shown that the absorption bands of the PS matrix were not affected by the encapsulated TiO₂ particles. It concluded that the TiO₂ was presented in PS hybrids.

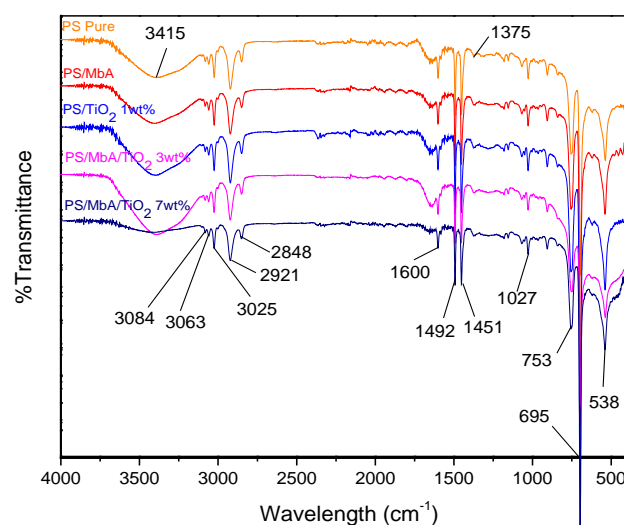


Figure 1 FT-IR spectra of PS, PS/MbA/TiO₂ with various 1-7 wt% TiO₂ contents.

FE-SEM was employed to observe the morphology of the PS hybrids. Figure 2 demonstrates the SEM images of PS hybrid TiO₂ 1, 3, and 7 wt% and their particle size distribution. The result shows that the particle diameter of the PS/MbA was 76 nm, as presented in Figure 2a. Moreover, the PS/MbA/TiO₂ 1 and 3 wt% were similar at 88 nm, as shown in Figures 2c and 2e. For 7 wt% TiO₂ in Figure 2g, the particle diameter of PS/MbA/TiO₂ was increased to 95 nm, which increased by 25%. The particle size distribution of the PS and PS hybrids demonstrated

a narrow size distribution, as seen in Figures 2b, 2d, and 2f. It concludes that the encapsulation of TiO₂ in the PS mini-emulsion caused an increase in the

final particle size of the hybrid. This was due to an increase in the amount of TiO₂ in the PS hybrid [24].

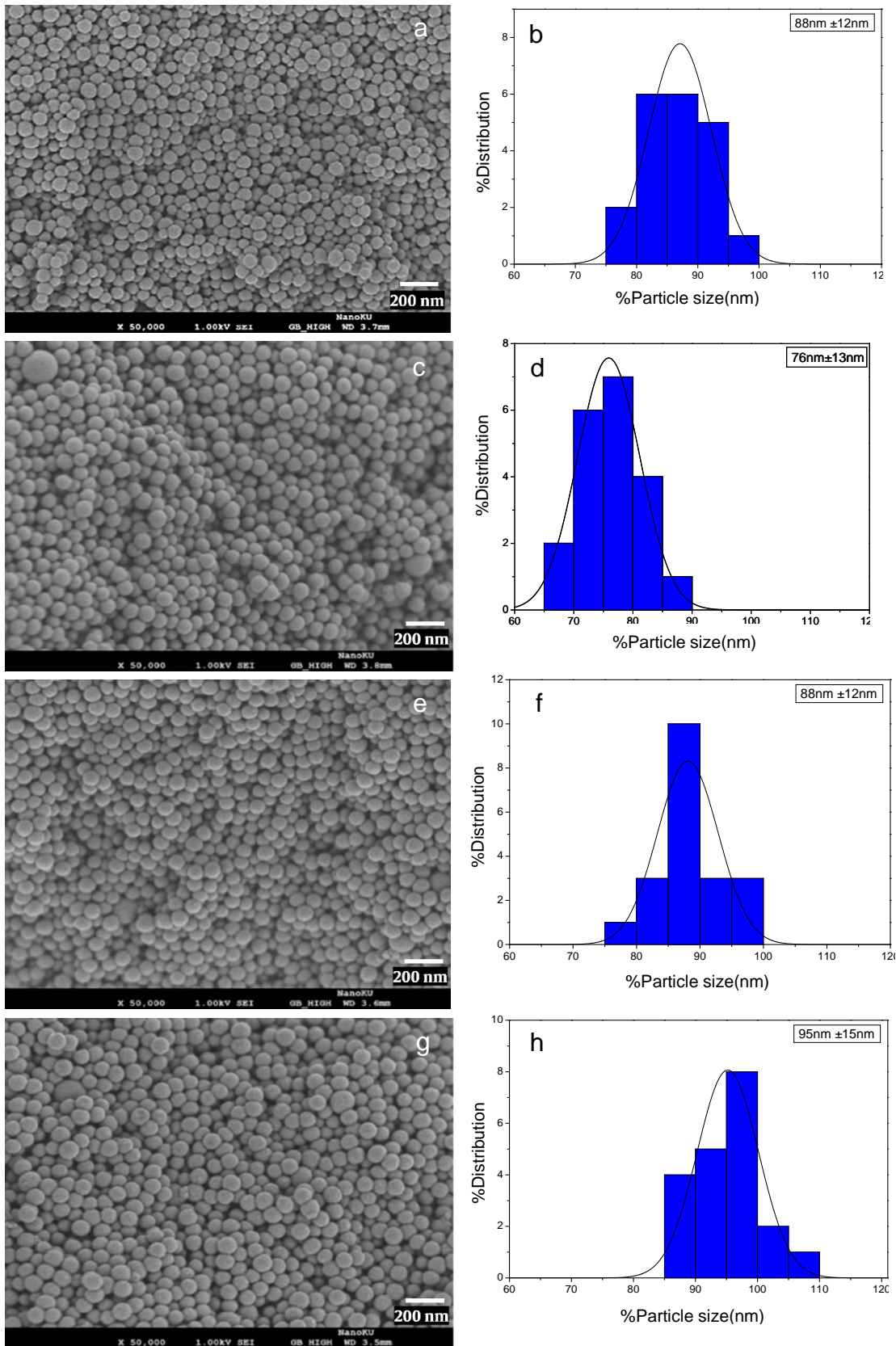


Figure 2 SEM images of PS hybrids and their particle size distribution of (a-b) PS, (c-d) PS/MbA/TiO₂ 1 wt%, (e-f) PS/MbA/TiO₂ 3 wt%, and (g-h) PS/MbA/TiO₂ 7 wt%. The scale bar was 100 nm.

The HR-TEM was employed to demonstrate the morphology and crystalline structure of the PS hybrids. The sphere shape of the PS matrix was found with a few large particles due to the free radical polymerization, as seen in Figure 3a. Some TiO₂,

moreover, was encapsulated in the PS hybrid. Figure 3b presents the Fast Fourier Transform (FFT) image of PS/MbA/TiO₂ 7 wt% at magnification 500,000 which demonstrates the crystalline structure of TiO₂ (dot) and the amorphous structure of PS (ring).

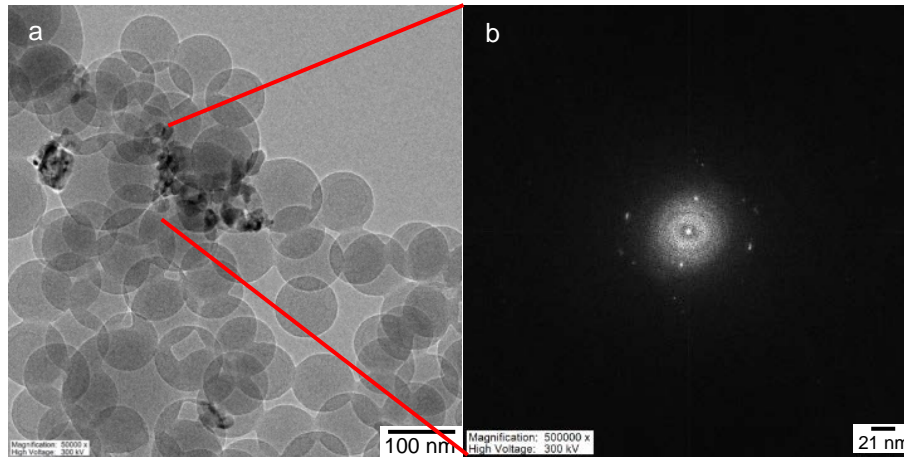


Figure 3 (a) HR-TEM image of PS/MbA/TiO₂ 7 wt%, (b) Fast Fourier Transform (FFT) of PS/MbA/TiO₂ 7 wt%.

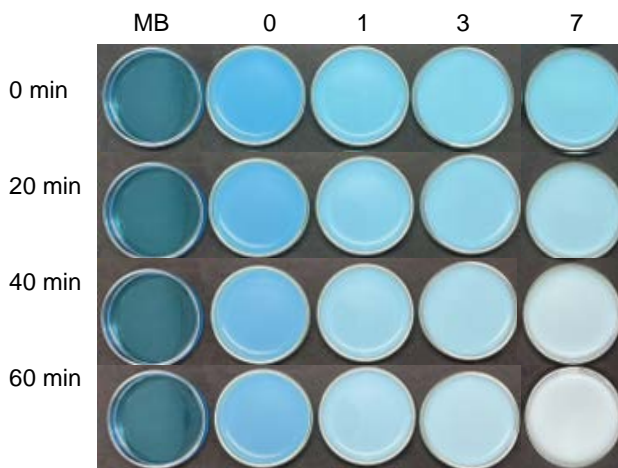


Figure 4 The discoloration of MB under UV light of PS/MbA/TiO₂ 0-7 wt% in 1 h.

Table 2 The Hunter L*, a*, b* color scale for PS/MbA/TiO₂ 0-7 wt% at 1 h.

PS/MbA/TiO ₂ 0 wt%	L*	a*	B*
0min	53.59	-10.89	-25.78
60min	54.15	-10.26	-23.87
PS/MbA/TiO ₂ 1 wt%	L*	a*	B*
0min	65.64	-15.38	-21.85
60min	65.51	-13.94	-19.67
PS/MbA/TiO ₂ 3 wt%	L*	a*	B*
0min	69.89	-15.72	-19.00
60min	73.73	-11.24	-12.49
PS/MbA/TiO ₂ 7 wt%	L*	a*	B*
0min	73.52	-14.88	-15.67
60min	73.73	-11.24	-12.49

The photocatalytic activity of PS/MbA/TiO₂ 1-7 wt% was investigated by observing the discoloration of MB under UV light by measuring the Hunter L*, a*, b* color scales; for the "L*" scale a low number (0-50)

presents dark and a high number (51-100) presents light. For the "a*" scale a positive number presents red and a negative number presents green. For the "b*" scale a positive number presents yellow and a negative number presents blue. Figure 4 demonstrates the discoloration of MB of PS/MbA/TiO₂ (0-7 wt%) for 1 h. It was found that the color of MB for PS/MbA was not changed due to the absence of a catalyze. For 1 wt% and 3 wt% of TiO₂ in PS hybrid, the MB color was slightly decreased, as seen in Figure 4. Table 2 shows the Hunter L*, a*, b* color scales for PS hybrids at 60 minutes. The result shows that in all the samples at 0 minute the L* was different due to the various amounts of white TiO₂. The negative b* scale was focused on due to the indicated blue color of MB. The b* value of the PS/MbA/TiO₂ 7 wt% was higher than PS/MbA due to the photocatalytic activity of the TiO₂ hybrid, as shown in Table 2. Moreover, the a* value is presented as less negative than increasing the photocatalytic degradation. An increased amount of TiO₂ improved the photocatalytic efficiency. It concludes that the TiO₂ was successfully integrated with PS nanoparticles via mini-emulsion and showed photocatalytic properties.

CONCLUSION

A Polystyrene (PS)/nano-TiO₂ hybrid was successfully investigated by the mini-emulsion process. To study the effect of crosslinking agents on the photocatalytic properties of the hybrid, *N,N*-methylenebis (acrylamide) (MbA) was added to the colloid system. The diameter, morphology, and photocatalytic properties of the samples were characterized and discussed. It was noticed that the 7 wt% TiO₂-PS/0.25 wt% MbA hybrid gives the highest photocatalytic properties. The FE-SEM confirmed the well-defined structure with a spherical shape and

network formation to improve the photocatalytic properties. The diameter and morphology of the PS/TiO₂ hybrid were in the range of 76 nm to 95 nm. In addition, the encapsulation of TiO₂ in the PS hybrid may result in an increase in the particle size of the hybrid. FT-IR spectroscopy was employed to analyze the functional group and bonding of the PS hybrid. The results showed that the absorption bands of the PS matrix were not affected by the encapsulated TiO₂ particles. It could be confirmed that the TiO₂ was encapsulated in PS hybrids. HR-TEM image of the PS/TiO₂ hybrid was studied to confirm the encapsulation of TiO₂ particles in the hybrid. It was noticed that the TiO₂ particles were successfully encapsulated in the PS/TiO₂ hybrid.

ACKNOWLEDGEMENT

This research was supported by The Science, Research and Innovation Promotion Funding (TSRI) (Grant no. FRB650070/0168). This research block grant was managed under Rajamangala University of Technology Thanyaburi (FRB65E0703E.1).

REFERENCES

- Selvin TP, Kuruvilla J, Sabu T. Mechanical properties of titanium dioxide-filled polystyrene microcomposites. *Mater Lett.* 2004;58(3):281-9.
- Sanchez C, Julián B, Belleville P, Popall M. Applications of hybrid organic-inorganic nanocomposites. *J Mater Chem.* 2005;15(3536):3559-92.
- Lebeau B, Sanchez C. Sol-gel derived hybrid inorganic-organic nanocomposites for optics. *Curr Opin Solid State Mater Sci.* 1999;4(1):11-23.
- Kim TW, Yang Y, Li F, Kwan WL. Electrical memory devices based on inorganic/organic nanocomposites. *NPG Asia Mater.* 2012;4(6):e18-e.
- Jordan J, Jacob KI, Tannenbaum R, Sharaf M, Jasiuk I. Experimental trends in polymer nanocomposites - a review. *Mater Sci Eng.* 2009;393:1-11.
- Amin KF, Asrafuzzaman, Nahin AM, Hoque ME. 10 - Polymer nanocomposites for adhesives and coatings. In: Hoque ME, Ramar K, Sharif A, editors. *Advanced Polymer Nanocomposites*: Woodhead Publishing; 2022. p. 235-65.
- Alam MR, Islam T, Repon MR, Hoque ME. 16 - Carbon-based polymer nanocomposites for electronic textiles (e-textiles). In: Hoque ME, Ramar K, Sharif A, editors. *Advanced Polymer Nanocomposites*: Woodhead Publishing; 2022. p. 443-82.
- Wang X, Wang X, Meng A, Li Z, Xing J. Rapid, continuous, large-scale synthesis of ZnO/Ag hybrid nanoparticles via one-step impinging stream route for efficient photocatalytic and anti-algal applications. *Mater Today Commun.* 2022;30:103121.
- Ferreira Soares DC, Domingues SC, Viana DB, Tebaldi ML. Polymer-hybrid nanoparticles: Current advances in biomedical applications. *Biomed Pharmacother.* 2020;131:110695.
- Shetty A, Chandra S. Inorganic hybrid nanoparticles in cancer theranostics: understanding their combinations for better clinical translation. *Mater Today Chem.* 2020;18:100381.
- Fitriani F, Bilad MR, Aprilia S, Arahman N. Biodegradable Hybrid Polymer Film for Packaging: A review. *J Nat Fibers.* 2023;20(1):2159606.
- Lan Y, Lu Y, Ren Z. Mini review on photocatalysis of titanium dioxide nanoparticles and their solar applications. *Nano Energy.* 2013;2(5):1031-45.
- Metanawin S, Metanawin T. Fabrication of hybrid polystyrene-titanium dioxide with enhanced dye degradation and antimicrobial properties: investigation of the effect of triethylene glycol dimethacrylate on photocatalytic activity. *Polym Int.* 2022;71(7):777-89.
- Metanawin S, Sornsuwit N, Metanawin T. Miniemulsion polymerization technique enhancement: The photocatalysis of commercial rutile-TiO₂ hybrids with nano poly(methyl methacrylate). *Polym-Plast Technol Mater.* 2022;61(1):56-68.
- Metanawin T, Panutumrong P, Metanawin S. Synthesis of Polyurethane/TiO₂ Hybrid with High Encapsulation Efficiency Using One-Step Miniemulsion Polymerization for Methylene Blue Degradation and its Antibacterial Applications. *ChemistrySelect.* 2023;8(11):e202204522.
- Sztorch B, Nowak K, Frydrych M, Leśniewska J, Krysiak K, Przekop RE, et al. Improving the Dispersibility of TiO₂ in the Colloidal System Using Trifunctional Spherosilicates. *Materials.* 2023;16(4):1442.
- Akhtar S, Shahzad K, Mushtaq S, Ali I, Rafe MH, Fazal-ul-Karim SM. Antibacterial and antiviral potential of colloidal Titanium dioxide (TiO₂) nanoparticles suitable for biological applications. *Mater Res Express.* 2019;6(10):105409.
- Tsang CHA, Li K, Zeng Y, Zhao W, Zhang T, Zhan Y, et al. Titanium oxide based photocatalytic materials development and their role of in the air pollutants degradation: Overview and forecast. *Environ Int.* 2019;125:200-28.

19. Fujishima A, Rao TN, Tryk DA. Titanium dioxide photocatalysis. *J Photochem Photobiol C*. 2000; 1(1):1-21.
20. Reddy KR, Hassan M, Gomes VG. Hybrid nanostructures based on titanium dioxide for enhanced photocatalysis. *Appl Catal A: Gen*. 2015;489:1-16.
21. Mironyuk IF, Soltys LM, Tatarchuk TR, Tsinurchyn VI. Ways to Improve the Efficiency of TiO₂-based Photocatalysts (Review). *Phys Chem Solid State*. 2020;21(2):300-11.
22. Rong Y, Chen HZ, Wu G, Wang M. Preparation and characterization of titanium dioxide nanoparticle/polystyrene composites via radical polymerization. *Mater Chem Phys*. 2005;91(2):370-4.
23. Melgoza-Ramírez ML, Ramírez-Bon R. Microstructural comparison between PMMA-SiO₂ and PMMA-TiO₂ hybrid systems using Eu³⁺ as ion-probe luminescence. *J Non-Cryst Solids*. 2020;544:120167.
24. Erdem B, Sudol ED, Dimonie VL, El-Aasser MS. Encapsulation of inorganic particles via miniemulsion polymerization. *Macromol Symp*. 2000;155(1): 181-98.